Journal of Alloys and Compounds 496 (2010) 226–233

Contents lists available at ScienceDirect

Journal of Alloys and Compounds

journal homepage: www.elsevier.com/locate/jallcom

Review

Ab-initio investigation of structural, electronic and optical properties of $In_xGa_{1-x}As$, $GaAs_{1-y}P_y$ ternary and $In_xGa_{1-x}As_{1-y}P_y$ quaternary semiconductor alloys

M. Othman*, E. Kasap, N. Korozlu

Gazi University, Department of Physics, Teknikokullar, 06500 Ankara, Turkey

ARTICLE INFO

Article history:
Received 15 September 2009
Received in revised form
14 December 2009
Accepted 18 December 2009
Available online 24 December 2009

Keywords:
Semiconductor alloys
Electronic properties
Optical properties

ABSTRACT

The structural, electronic and optical properties of $In_xGa_{1-x}As$, $GaAs_{1-y}P_y$ ternary and $In_xGa_{1-x}As_{1-y}P_y$ quaternary semiconductor alloys are investigated using first-principles plane-wave pseudo-potential method within the LDA approximations. For these alloys lattice parameters, bulk modulus, band gap energy and density of states are calculated. Besides, we have calculated the optical parameters (dielectric functions, energy loss function, reflectivity, absorption and refractive index) of these semiconductor alloys. Our results agree well with the available theoretical and experimental data in the literature.

© 2010 Elsevier B.V. All rights reserved.

Contents

1. Introduction 226
2. Method of calculation 227
3. Results and discussion 229
   3.1. Structural and electronic properties 229
   3.2. Optical properties 229
4. Conclusions 232
   Acknowledgements 232
   References 232

1. Introduction

At present, III–V compound semiconductors provide the material basis for a number of well-established commercial technologies, as well as new cutting-edge classes of electronic and optoelectronic devices. Only a few examples include high-electron-mobility and heterostructure bipolar transistors, diode lasers, light-emitting diodes, photodetectors, electro-optic modulators, and frequency-mixing components [1–4]. The operating characteristics of these devices depend critically on the physical properties of the constituent materials, which are often combined in quantum heterostructures containing carriers confined to dimensions on the order of a nanometer. A seemingly limitless flexibility is now available to the quantum heterostructure device designer [5]. Semiconductors are tremendously important both technologically and economically [6–12]. Semiconductors with predictable and reliable electronic properties are necessary for mass production. The level of chemical purity is extremely high because even small number of impurities can have big effects on the properties of the material. A high degree of crystalline perfection is also required, since faults in crystal structure (such as dislocations, twins and stacking faults) interfere with the semiconducting properties of the material. Semiconductor alloys are made of elements from Group III and Group V on the periodic table such as gallium arsenide (GaAs) and indium phosphide (InP), which are used to emit light in typical optical devices. It is devoted to the description of the structural lattice, structural electronic energy-band, optical and carrier transport properties of these semiconductors. Some corrective effects

* Corresponding author. Tel.: +90 312 202 36 83; fax: +90 312 212 22 79.
E-mail address: mazin@gazi.edu.tr (M. Othman).

0925-8388/$ – see front matter © 2010 Elsevier B.V. All rights reserved.
doi:10.1016/j.jallcom.2009.12.109

and related properties, such as piezoelectric, elasto-optical and electro-optical properties, are also discussed. In particular, compound semiconductors are extremely efficient in generating light from electricity and converting light back into electricity. Therefore they have been the key materials for semiconductor lasers, LEDs and detectors [13]. These are in the heart of nearly all optoelectronic systems, including fiber-optic communication, optical storage display technology and satellite power systems. These semiconductor materials can be crystallized in either the cubic zinc-blende (sphalerite) (beta) phase or the hexagonal wurtzite (alpha) phase, but, for each material, one or the other of those phases is thermodynamically more stable at 300 K, as indicated. Wurtzite structure is applied due to its direct energy band gap in III–V semiconductors. The III–V semiconductor ternary alloys which are often used today include InGaAs, AlGaAs, InGaP, InGaN, and InAsP. In a more general sense, it belongs to the InGaAsP quaternary system that consists of alloys of indium arsenide (InAs), gallium arsenide (GaAs), indium phosphide (InP), and gallium phosphide (GaP). As gallium and indium belong to Group III of the periodic table, and arsenic and phosphorous belong to Group V, these binary materials and their alloys are all Group III. To a large extent, the electrical and optical properties of a semiconductor depend on its energy band gap and whether the band gap is "direct" or "indirect". The energy band gaps of the 4 binary members of the InGaAsP quaternary system range from 0.33 eV (InAs) to 2.25 eV (GaP), with InP (1.29 eV) and GaAs (1.43 eV) falling in between. A semiconductor will only detect light with photon energy larger than the band gap, in other words, with a wavelength shorter than the cutoff wavelength associated with the band gap. This "long wavelength cutoff" works out to 3.75 μm for InAs and 0.55 μm for GaP with InP at 0.96 μm and GaAs at 0.87 μm [14,15]. The operating characteristics of these devices depend critically on the physical properties of the constituent materials, which are often combined in quantum heterostructures, containing carriers confined to dimensions on the order of a nanometer. A seemingly limitless flexibility is now available to the quantum heterostructure device designer. $In_xGa_{1-x}As$, $GaAs_{1-y}P_y$ ternary and $In_xGa_{1-x}As_{1-y}P_y$ quaternary semiconductor alloys have been the subject of various experimental and theoretical studies recently and in the past decades. John [16] studied first-principles calculation of semiconductor-alloy phase diagrams. Zunger [17] studied spatial correlations in GaInAsN alloys and their effects on band-gap enhancement and electron localization. Clint [18] studied computational band-structure engineering of III–V semiconductor alloys.

Today, the production and the use with technological devices of GaAs-based, In and P have added semiconductors, which become more important gradually and increase more and more. Experimental studies on such type of produced semiconductor alloys are carried out intensively.

This study was carried out to shed light on the future studies of scientists who experimentally prepare and test these alloys in laboratories, to help them in determining the change in amounts of additives in alloys, and to determine the accordance of theoretical studies with experiments and other theoretical works. To this end, features of new semiconductor alloys that may be obtained by adding In and P to GaAs structure at various ratios were examined.

In this work, we used the Cambridge serial total energy package (CASTEP) code [19] to study the structural, electronic and optical properties, such as band structures, dielectric functions and energy loss functions, respectively, absorption of $In_xGa_{1-x}As$, $GaAs_{1-y}P_y$ ternary and $In_xGa_{1-x}As_{1-y}P_y$ quaternary alloys. The results of our calculation of the lattice constants and the energy gaps agree well with the previous theoretical study. In addition, the optical properties of the compounds with respect to the band gap changing with the molar fraction (x and y) of each $In_xGa_{1-x}As$, $GaAs_{1-y}P_y$ and $In_xGa_{1-x}As_{1-y}P_y$ are studied not only to enrich the fundamental understanding of barium chalcogenides, but also to complement the research of all the chalcogenides as well as the total III–V compounds. For these alloys lattice parameters, bulk modulus, band gap energy and density of states are calculated. Besides, we have calculated the optical parameters (energy loss function, reflectivity, absorption and refractive index) of these semiconductor alloys.

2. Method of calculation

The physical properties of $In_xGa_{1-x}As$, $GaAs_{1-y}P_y$ ternary and $In_xGa_{1-x}As_{1-y}P_y$ quaternary alloys are investigated using the CASTEP program [19]. The model wurtzite is used in $In_xGa_{1-x}As$, $GaAs_{1-y}P_y$ ternary and $In_xGa_{1-x}As_{1-y}P_y$ quaternary alloys. We apply a 16-atom super cell which coressponds to a $2 \times 2 \times 1$ that is twice the size of the primitive wurtzite unit cell in basic plane direction. In this program the calculation is performed using Kohn–Sham formation [20], which is based on the density function theory (DFT). Local density approximation (LDA) is made for electronic exchange-correlation potential energy. Coulomb potential energy caused by electron–ion interaction is described using pseudo-potential concept. The optimized non-local pseudo-potential generated using the scheme proposed by Liuo et al. [21] and is adopted, in which tee orbitals of Ga ($3d^{10}4s^24p^1$), In ($4d^{10}5s^25p^1$), As ($4s^24p^3$) and P ($3s^23p^3$) are treated as valence electrons. By the non-conserving condition, the pseudo-wave function is related to pseudo-potential matches and the plane-wave function expanded with Kohn–Sham formation beyond cutoff energy.

A cubic unit cell is constructed with four Group III atoms (Ga/In) and four Group V atoms (As). We have considered $In_xGa_{1-x}As$, $GaAs_{1-y}P_y$ ternary and $In_xGa_{1-x}As_{1-y}P_y$ quaternary alloys as having cubic symmetry in our calculation for all the five systems to maintain consistency and simplicity. We expect that for $x = 0.5$ the alloy is a layered structure and should be non-cubic. We have taken four layers and hence a cubic unit cell for $x = 0.25, 0.50, 0.75$ we have replaced one, two and three Ga atoms, respectively, by In to get the desired concentration. The idea of constructing an alloy by taking a large unit cell (cubic 8-atom) and repeating it three dimensionally for the calculation of the electronic structure of the semiconductor alloy has been used by Agrawal et al. [22]. Agrawal et al. [22] have used an 8-atom cubic super cell to calculate the electronic properties of $In_xGa_{1-x}As$ alloys, although no such calculations have been performed for $In_xGaIn_xGa_{1-x}As$, $GaAs_{1-y}P_y$ ternary and $In_xGa_{1-x}As_{1-y}P_y$ quaternary alloys. The wave functions are expanded in the plane waves up to a kinetic-energy cutoff of 880 eV. In this work, the k-points of $6 \times 6 \times 4$ for $x = 0.5$ and $4 \times 4 \times 4$ for the other compositions x and y. For each $In_xGa_{1-x}As$, $GaAs_{1-y}P_y$ and $In_xGa_{1-x}As_{1-y}P_y$ in this study, once the ratio between the In, Ga, As and P atoms is specified, the CASTEP simulation program randomly determines the geometrical arrangement of In–Ga and As–P atoms. In this simulation program, the chosen structural properties are the equilibrium lattice constant (a_0), bulk modulus (B_0), the energy gap at the Γ point (E_g) and optical constant for crystalline GaAs, InAs, GaP, InP, $In_xGa_{1-x}As$, $GaAs_{1-y}P_y$ and $In_xGa_{1-x}As_{1-y}P_y$ in the bulk structure using electronic exchange correlation energy.

Geometry optimization is performed for $In_xGa_{1-x}As$, $GaAs_{1-y}P_y$, $In_xGa_{1-x}As_{1-y}P_y$ with symmetry P1. Atomic positions are relaxed and optimized with a density mixing scheme [23] using the conjugate-gradient (CG) method [24] for eigenvalues minimization. The iteration is repeated until the energy is less than 0.002 meV/atom and the RMS stress is less than 0.1 GPa. The Monkhorst-Pack scheme [25] with uniform mesh points is applied.

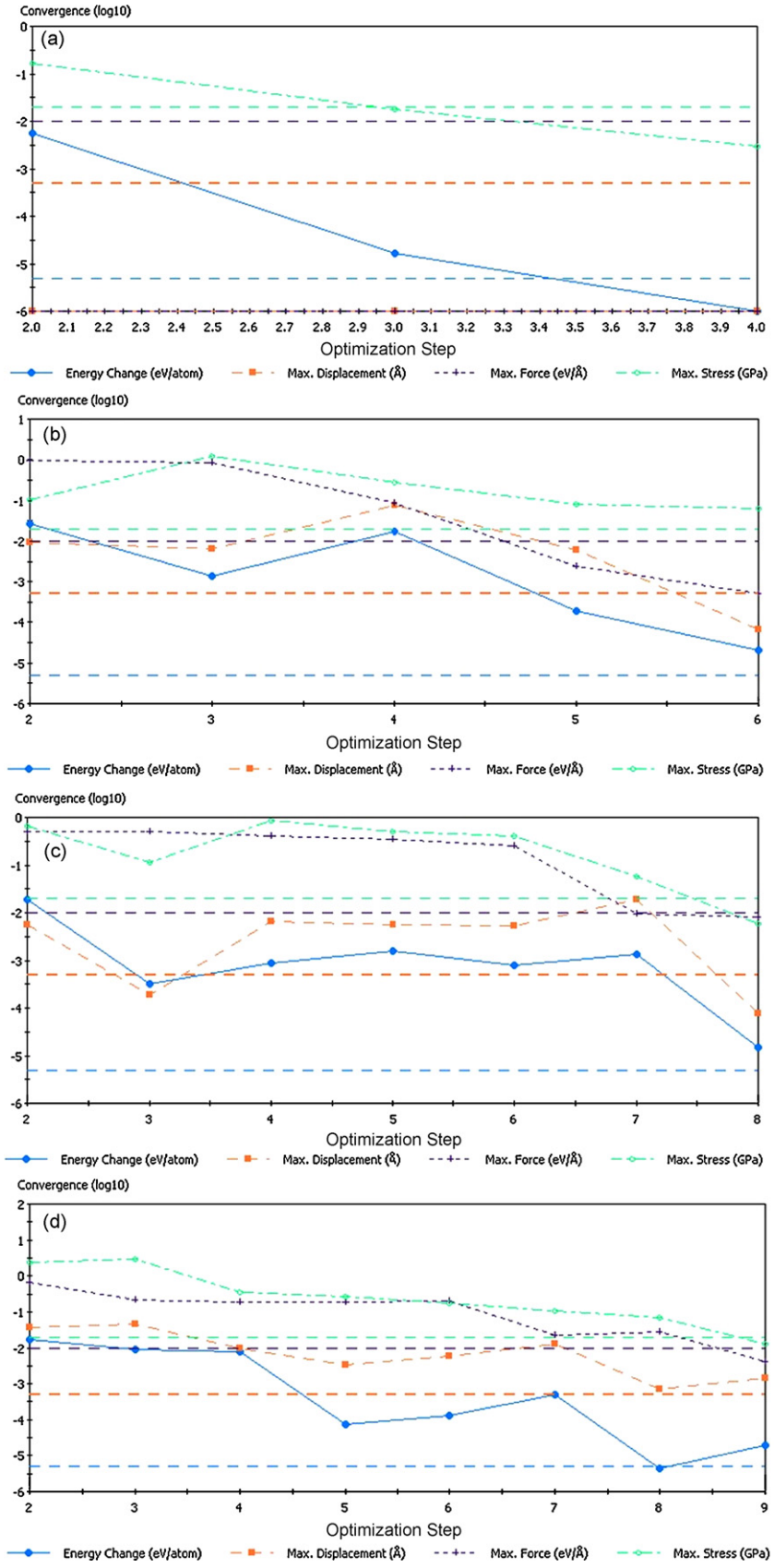

Fig. 1. The optimization setup convergence of (a) GaAs, (b) In_xGa_{1-x} As, (c) $GaAs_{1-y}P_y$ and (d) $In_xGa_{1-x}As_{1-y}P_y$.

3. Results and discussion

3.1. Structural and electronic properties

As in the first step in calculations, the lattice constants of alloys at equilibrium are calculated by minimizing the lattice parameter of the crystal, i.e. the ratio of total energy of the crystal to its volume. The tested optimization setup convergence is shown in Fig. 1(a–d). Bulk module is also calculated for each structure. With these calculated values, lattice parameters and bulk modulus having values of x and $y = 0$, 0.25, 0.5, 0.75 and 1 for $In_xGa_{1-x}As$, $GaAs_{1-y}P_y$ ternary alloys and $In_xGa_{1-x}As_{1-y}P_y$ quaternary alloys were calculated as a function of In and P composition rates for GaAs having zinc-blende structure. These obtained results are compared with other theoretical and experimental studies. It is found out that the lattice constant for GaAs is 0.5% greater than theoretical value [26,27] and 2% less than experimental value [28]. The minimum value of lattice constant a_0 is obtained as 5.58 Å for GaAs structure and the maximum value is obtained as 5.82 Å for $In_xGa_{1-x}As$. It is found out that the calculated bulk module is 1% less than the theoretical value. Here, the results of lattice parameters only for x and $y = 0.5$ are given in Table 1 together with the other studies in order to save pages.

In the present case the bulk modulus of $In_xGa_{1-x}As$, $GaAs_{1-y}P_y$ ternary and $In_xGa_{1-x}As_{1-y}P_y$ quaternary alloys were studied as a function of x and y (x, $y = 0$, 0.25, 0.50, 0.70 and 1) composition. It is seen that the compressibility, according to the decreasing value of x and y, is changing in the following sequence:

$$GaAs > In_{0.25}Ga_{0.75}As > In_{0.5}Ga_{0.5}As > In_{0.75}Ga_{0.25}As > InAs$$

$$GaAs < GaAs_{0.75}P_{0.25} > GaAs_{0.5}P_{0.5} > GaAs_{0.75}P_{0.25} < InP$$

$$GaAs < In_{0.25}Ga_{0.75}As_{0.75}P_{0.25} > In_{0.5}Ga_{0.5}As_{0.5}P_{0.5} < In_{0.5}Ga_{0.5}As_{0.5}P_{0.5}$$

Using the lattice constants calculated at equilibrium state for the studied alloys, the electronic band structures corresponding to high symmetry points are obtained. Fermi level is adjusted as the zero energy level. At the same time, the total densities of states (DOS) for these alloys are calculated. For the sake of saving pages, here the band structure only for $In_{0.5}Ga_{0.5}As$ alloy is given in Fig. 2.

As a result of the drawn band structures, it is found out that these structures have direct band range at Γ symmetry point at the center of Brillouin region. $GaAs_{1-y}P_y$ is a wide-band gap alloy that is often employed in red LEDs. The alloy has indirect band gap range for $y \geq 0.50$. The values of energy band range for each structure are taken from the obtained energy band structure table and these are presented in chart form in Fig. 3. The obtained values are

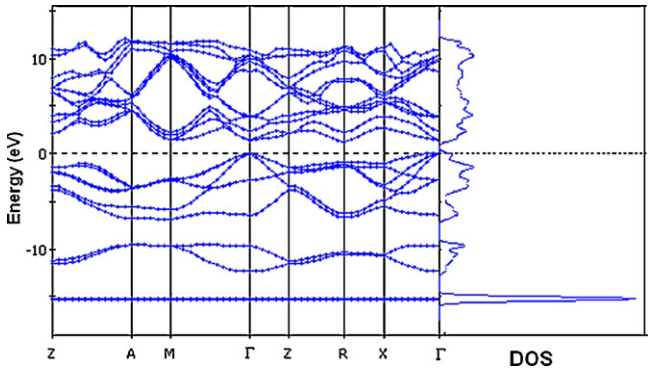

Fig. 2. Calculated band structure and DOS of $In_{0.5}Ga_{0.5}As$.

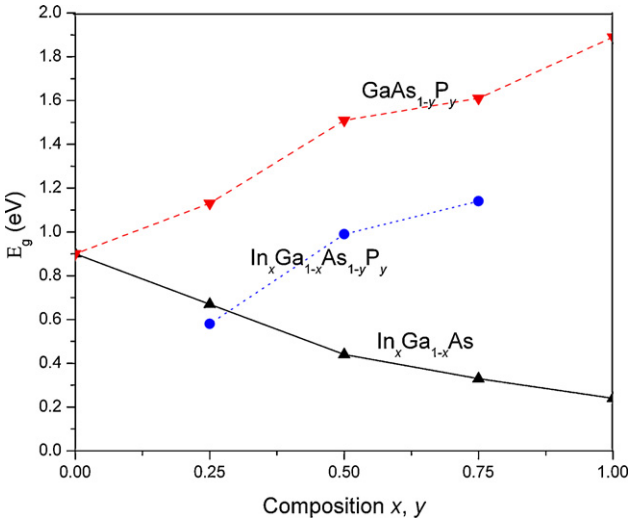

Fig. 3. Band gap energies of $In_xGa_{1-x}As$, $GaAs_{1-y}P_y$ and $In_xGa_{1-x}As_{1-y}P_y$.

found to be in compliance with the theoretical results [23,27–30] and to be less than the experimental results [31,32]. This is caused by the discontinuity of exchange energy in the calculations of density functional theory. Scissors process is required to align the band range with the experimental results.

Fig. 3 shows band gap for $In_xGa_{1-x}As$, $GaAs_{1-y}P_y$ ternary alloys and $In_xGa_{1-x}As_{1-y}P_y$ quaternary alloys as a function of x and y compositions. $In_xGa_{1-x}As$ alloy the optical band gap decreases from 0.9 to 0.24 eV with increasing In concentrations and in $GaAs_{1-y}P_y$ alloy, the optical band gap increases from 0.9 to 1.89 eV with increasing P concentrations. In $In_xGa_{1-x}As_{1-y}P_y$ quaternary semiconductor alloys the optical band gap increases from 0.48 to 1.10 eV with increasing In and P concentrations. The band gaps are smaller than the experimental values [31,32] because of the use of the LDA in our calculations. However, it should be explained that the LDA correction is neither constant nor does it vary linearly with the size of the band gap.

3.2. Optical properties

When a photon is sent on a semiconductor, certain optical events, such as absorption, transition, reflection and refraction, take place as a result of interaction between atom electrons with photons [33]. If the photons that are sent on the material do not have sufficient energy to excite the electron to a higher energy level, then instead of being absorbed, they pass through material that behaves as transparent. Therefore, semiconductors behave as absorbers for short wavelength photons and as transparent for very long wavelength photons [34]. Absorption or transition of a photon depends on the photon's energy, prohibited energy range of semiconductor and the arrangement of atoms [35]. The optical constants, such as absorption, loss function and refractive index are very important for the optical materials and related applications.

To investigate the optical band gap and optical transition of the GaAs, $In_xGa_{1-x}As$, $GaAs_{1-y}P_y$ ternary and $In_xGa_{1-x}As_{1-y}P_y$ system, it is necessary to investigate the imaginary part of the dielectric function $\varepsilon_2(\omega)$ because $\varepsilon_2(\omega)$ is very important for the optical properties of some materials. It is well-known that the interaction of a photon with the electrons in the system can be described in terms of time dependent perturbations of the ground-state electronic states. Optical transitions between occupied and unoccupied states are caused by the electric field of the photon. The spectra from the excited states can be described as a joint DOS between the valence and conduction bands. The momentum matrix elements, which are

Table 1
Calculated equilibrium lattice constants (a_0), bulk modulus (B) and results of other experimental and theoretical works of GaAs, $In_{0.5}Ga_{0.5}As$, $GaAs_{0.5}P_{0.5}$ and $In_{0.5}Ga_{0.5}As_{0.5}P_{0.5}$.

Materials	Structure	Reference	a_0 (Å)	b_0 (Å)	c_0 (Å)	B (GPa)
GaAs	Zinc-blende	Present	5.58	–	–	74.53
		Theory[a]	5.53	–	–	75.73
		Theory[b]	5.54	–	–	77.10
		Expt.[c]	5.64	–	–	77.00
$In_{0.5}Ga_{0.5}As$	Tetragonal *P*-4*m*2	Present	5.82	4.90	4.90	66.45
		Theory[a]	5.75	4.8	4.80	–
$GaAs_{0.5}P_{0.5}$	Tetragonal *P*-4*m*2	Present	5.73	3.87	3.87	85.30
$In_{0.5}Ga_{0.5}As_{0.5}P_{0.5}$	Orthorombic *P*2221	Present	5.64	5.67	5.64	80.35

[a] Ref. [26].
[b] Ref. [27].
[c] Ref. [28].

used to calculate the $\varepsilon_2(\omega)$, are calculated between occupied and unoccupied states, which are given by the eigenvectors obtained as the solution of the corresponding Schrodinger equation. Evaluating these matrix elements, one uses the corresponding eigenfunctions of each of the occupied and unoccupied states.

Using the DFT, the electronic excitability spectrum of a material is generally defined according to the complex dielectric function based on frequency: $\varepsilon(\omega) = \varepsilon_1(\omega) + i\varepsilon_2(\omega)$ Both the real part and the imaginary part of complex dielectric function are based on frequency containing all of the desired reaction information. These real and imaginary parts are correlated with Kramers–Kronig correlations:

$$\varepsilon_1(\omega) = 1 + \frac{2}{\pi}\int_0^{\infty} \frac{\varepsilon_2(\omega')\omega' d\omega'}{\omega'^2 - \omega^2} \tag{1}$$

$$\varepsilon_2(\omega) = \frac{Ve^2}{2\pi\hbar m^2\omega^2}\int d^3k \sum_{nn'} \left|\left\langle kn\right| p \left|kn'\right\rangle\right|^2 f(kn) \times \left[1 - f(kn')\right]\delta(E_{kn} - E_{kn'} - \hbar\omega) \tag{2}$$

Since the optical properties of a solid are the reactions of electrons to the time dependent electromagnetic perturbation caused by the light absorbed, the calculation of the optical properties of the solid means calculation of the optical reaction function, i.e. the complex dielectric function. Some optical constants can also be calculated using the dielectric function [36–38]. Real components of the function can be obtained with the help of imaginary components of dielectric function, energy loss function, refraction index n and attenuation coefficient k which are determined with the components of dielectric tensor:

$$n(\omega) = \frac{1}{\sqrt{2}}\left[\sqrt{\varepsilon_1^2(\omega) + \varepsilon_2^2(\omega) + \varepsilon_1}\right]^{1/2} \tag{3}$$

$$k(\omega) = \frac{1}{\sqrt{2}}\left[\sqrt{\varepsilon_1^2(\omega) + \varepsilon_2^2(\omega) + \varepsilon_1}\right]^{1/2} \tag{4}$$

$$L(\omega) = -Im\left(\frac{1}{\varepsilon}\right) = \frac{\varepsilon_2(\omega)}{[\varepsilon_1^2(\omega) + \varepsilon_2^2(\omega)]} \tag{5}$$

$$\alpha(\omega) = \sqrt{2\omega}\left[\sqrt{\varepsilon_1^2(\omega) + \varepsilon_2^2(\omega)} - \varepsilon_1(\omega)\right]^{1/2} \tag{6}$$

$$R(\omega) = \left[\frac{\sqrt{\varepsilon_1^2(\omega) + j\varepsilon_2^2(\omega)} - 1}{\sqrt{\varepsilon_1^2(\omega) + j\varepsilon_2^2(\omega)} + 1}\right]^2 \tag{7}$$

In this section of the study, optical properties of the alloy for each structure according to x and y values are examined using the pseudo potentials produced with the DFT. Since Kohn–Sham equations determine only the fundamental status properties, it does not make sense to consider unoccupied levels in calculations; however, in order to calculate optical properties, transmission bands should be considered. In order to get rid of this discrepancy, "*scissors operator*" is used to render the experimental and theoretical identical band ranges. The optical properties only for the value x and $y = 0.5$ of $In_xGa_{1-x}As$, $GaAs_{1-y}P_y$ ternary and $In_xGa_{1-x}As_{1-y}P_y$ quaternary alloys are based on In and P addition of GaAs structures which are given in comparison in this article.

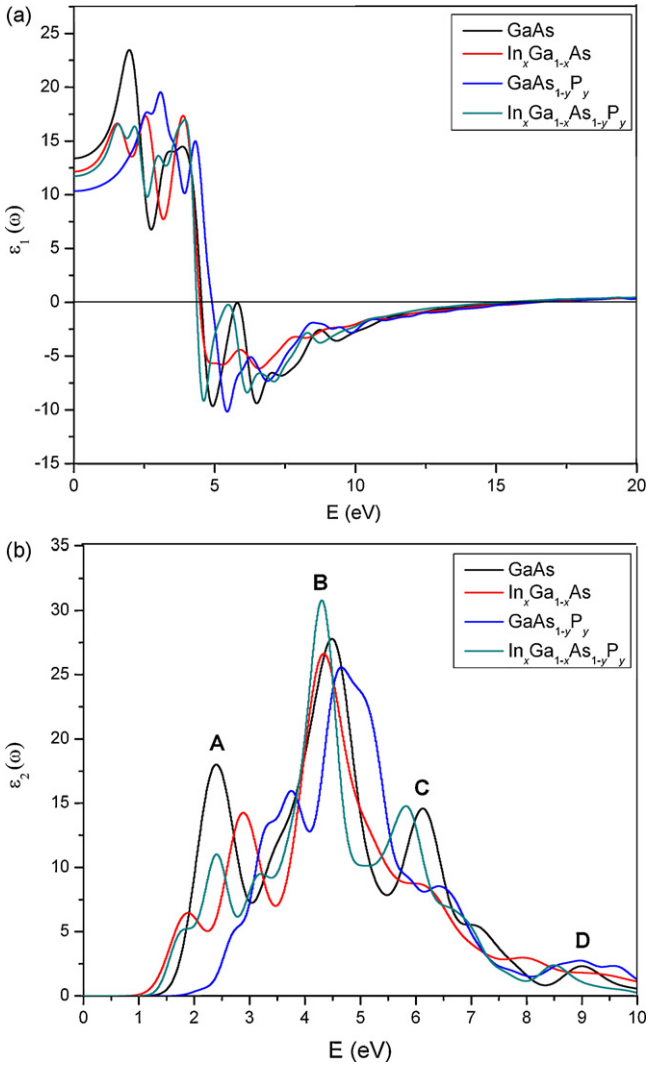

Fig. 4. (a) The real and (b) imaginary parts of dielectric function.

Table 2
Comparison of the interband contribution of the optical dielectric constant and high frequency dielectric constant.

Materials	Reference	$\varepsilon_1(0)$	ε_∞
GaAs	Present	13.40	0.65
	Theory[a]	10.90	–
	Expt.[b]	10.90	–
$In_{0.5}Ga_{0.5}As$	Present	14.60	0.30
	Theory[c]	13.10	–
$GaAs_{0.5}P_{0.5}$	Present	09.10	0.61
$In_{0.5}Ga_{0.5}As_{0.5}P_{0.5}$	Present	11.21	0.54

[a] Ref. [5].
[b] Ref. [30].
[c] Ref. [31].

Fig. 4 shows the real and imaginary components of the linear dielectric function, for each structure, it is based on the photon energy of alloys calculated at cubic and tetragonal phases. With the help of these obtained functions, the energy loss function coefficient $L(\omega)$, refraction index $n(\omega)$, extinction coefficient $k(\omega)$, absorption coefficient $\alpha(\omega)$ and reflection $R(\omega)$ are calculated at two phases. The calculated values are compared with existing theoretical [26–28] and experimental [39–45] studies and it is found that there is a general harmony. In Fig. 3, the real and imaginary parts of x and $y = 0.5$ value dielectric function for $In_xGa_{1-x}As$, $GaAs_{1-y}P_y$ ternary and $In_xGa_{1-x}As_{1-y}P_y$ quaternary alloys formed based on In and P addition of GaAs structure, are given in comparison. The real part of the dielectric function Fig. 4(a) shows an increase with the increase in the photon energy out of the region between 2.1 and 5.3 eV and this is a normal dispersion. However, it decreases as the photon energy increases in the region between 2.1 and 5.3 eV. This is an abnormal dispersion characteristic. A strong absorption and an increase in reflection present at 2.0–5.3 eV photon-energy interval of GaAs structure. These semiconductors have fundamental absorption limit at Infrared spectrum regions. The significance of these regions increases especially for communication devices in device applications of such alloys. This will be seen in more detail in the absorption and reflectivity curves to be given later on. Static dielectric constant $\varepsilon_1(0)$ and high frequency dielectric constant ε_∞ of structures are calculated as seen in Fig. 3(a) and are given in Table 2.

The peak values of imaginary parts of dielectric function based on photon energy shown in Fig. 4(b) are given in Table 3. These peak values correspond to electronic passages from valence band to transmission band (optical transitions).

The shift in peak values depending on the composition value of GaAs structure is seen in Fig. 4(b). A change was observed in the peak values by adding In to the GaAs structure. The *A* peak values were observed to increase from 2.31 to 2.94 eV respectively (see Table 3). *C* and *D* peak values were found to increase. Peak values at point *B* that occurred depending on P composition ratio were observed to increase from 4.42 to 4.65 and decrease at point *D* from 8.9 to 8.1 eV respectively. Peak values which correspond to electronic transitions between bands were interpreted to change depending on In and P composition ratios.

Table 3
Comparative characteristics of linear optical functions of GaAs, $In_{0.5}Ga_{0.5}As$, $GaAs_{0.5}P_{0.5}$ and $In_{0.5}Ga_{0.5}As_{0.5}P_{0.5}$ alloys.

Peaks (eV)				
Materials	*A* (eV)	*B* (eV)	*C* (eV)	*D* (eV)
GaAs	2.31	4.42	6.11	8.9
$In_{0.5}Ga_{0.5}As$	2.94	4.40	6.24	–
$GaAs_{0.5}P_{0.5}$	3.74	4.65	6.40	8.81
$In_{0.5}Ga_{0.5}As_{0.5}P_{0.5}$	2.39	4.27	5.82	8.53

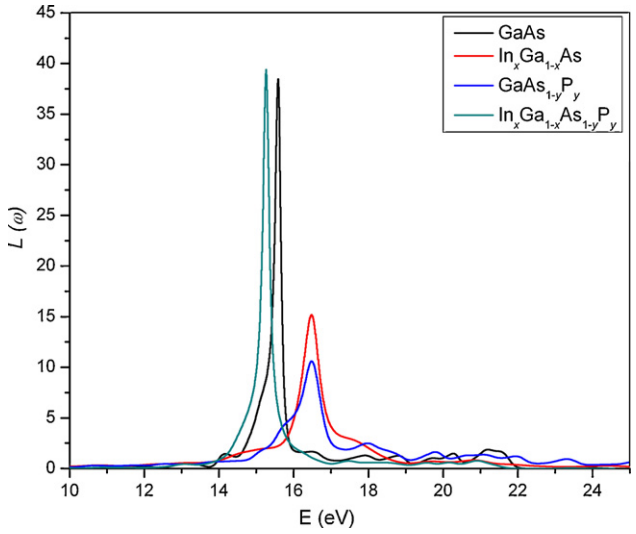

Fig. 5. Loss of function of GaAs, $In_{0.5}Ga_{0.5}As$, $GaAs_{0.5}P_{0.5}$ and $In_{0.5}Ga_{0.5}As_{0.5}P_{0.5}$ alloys.

Energy loss function defines the energy loss of the electrons passing between bands. Energy loss functions of alloys according to x and y values are calculated using Eq. (2). The definite maximums in energy loss function are related to collective vibrations of valence electrons. Consequently, as seen in Fig. 5, the energy loss function maximum at x and $y = 0.5$ of $In_xGa_{1-x}As$, $GaAs_yP_{1-y}$ ternary and $In_xGa_{1-x}As_yP_{1-y}$ quaternary alloys is based on In and P in addition GaAs structure has values 15.25, 16.48, 16.47 and 15.57 eV respectively. This is interpreted as the *plasma frequency* of peaks (Fig. 6).

Refraction indexes, which are calculated and based on photon energy of alloys using Eq. (4), are shown in Fig. 5, respectively for each structure. When the refraction indexes of GaAs, $In_{0.5}Ga_{0.5}As$, $GaAs_{0.5}P_{0.5}$ and $In_{0.5}Ga_{0.5}As_{0.5}P_{0.5}$ structures are compared with Fig. 5, the refraction indexes of alloys are found to be 3.81, 3.50, 3.20 and 3.47 respectively. These data and the calculated dielectric function results are found to be in compliance. Also, the extinction coefficients $k(\omega)$ calculated based on x and y compositions using Eq. (5) are given in Fig. 7 for each alloy.

Fig. 8 gives the optical absorption spectra of the GaAs, $In_{0.5}Ga_{0.5}As$, $GaAs_{0.5}P_{0.5}$ and $In_{0.5}Ga_{0.5}As_{0.5}P_{0.5}$ alloys under the scissor operation in the range of 0–7 eV. Due to the underestimation

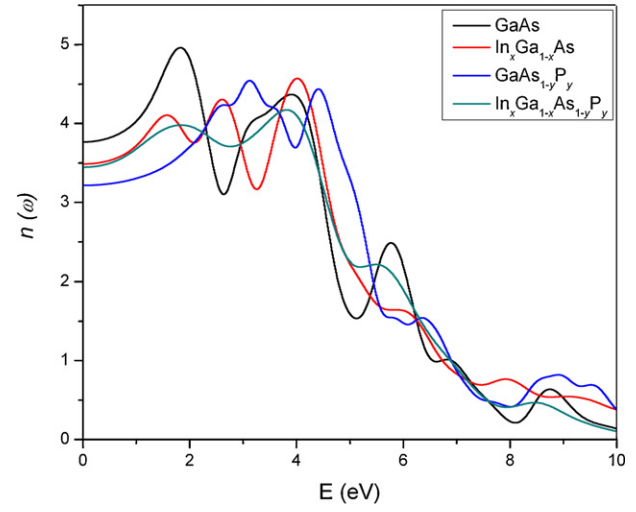

Fig. 6. Refractive index of GaAs, $In_{0.5}Ga_{0.5}As$, $GaAs_{0.5}P_{0.5}$ and $In_{0.5}Ga_{0.5}As_{0.5}P_{0.5}$ alloys.

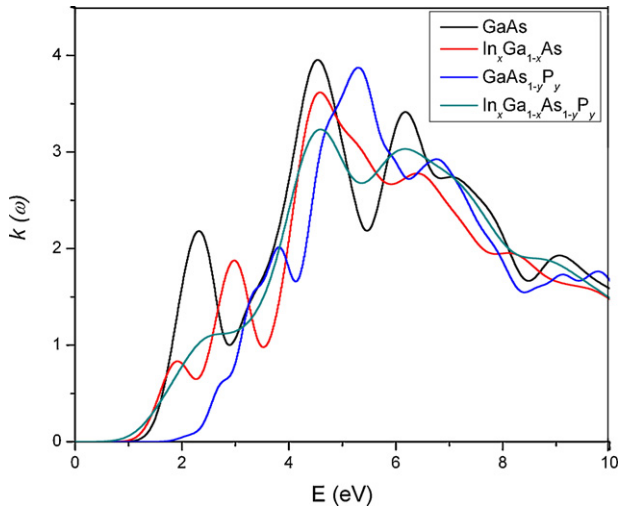

Fig. 7. Extinction coefficient $k(\omega)$ of GaAs, $In_{0.5}Ga_{0.5}As$, $GaAs_{0.5}P_{0.5}$ and $In_{0.5}Ga_{0.5}As_{0.5}P_{0.5}$ alloys.

of the band gap, it is difficult to obtain the exact optical band gap. In our calculations, we have used the energy scissor approximation with 1.43 eV to fit the absorption edge to the experimental value. This method is effective for a variety of systems [38]. The starting values of absorption are 1.43, 0.5, 1.80 and 1.31 eV respectively. It is well known that the relation between the optical band gap and the absorption coefficient is given by [46]

$$\alpha h\nu = c(h\nu - E_g)^{1/2} \quad (8)$$

where h is the Planck constant, c is the constant for a direct transition, ν is the frequency of radiation, and α is the optical absorption coefficient. The optical band gap E_g can be obtained from the intercept of $(\alpha h\nu)^2$ versus photon energy $(h\nu)$.

The reflectivity coefficients calculated using Eq. (7), are given in Fig. 8, based on x and y values for each structure. Reflectivity coefficients at x and $y = 0.5$ of $In_xGa_{1-x}As$, $GaAs_{1-y}P_y$ ternary and $In_xGa_{1-x}As_{1-y}P_y$ quaternary alloys are based on In and P addition of GaAs structure are given in comparison.

As seen in Fig. 9, the reflectivity of GaAs and $In_{0.5}Ga_{0.5}As_{0.5}P_{0.5}$ structures increase in the region between 2.30 and 8.5 eV. However, for $In_{0.5}Ga_{0.5}As$ and $GaAs_{0.5}P_{0.5}$ structures the increase in reflectivity is less than that of GaAs and $In_{0.5}Ga_{0.5}As_{0.5}P_{0.5}$. As seen in

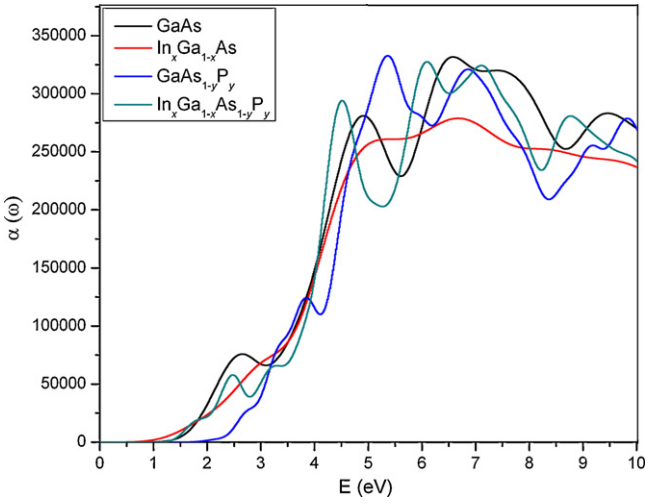

Fig. 8. Optical absorption of GaAs, $In_{0.5}Ga_{0.5}As$, $GaAs_{0.5}P_{0.5}$ and $In_{0.5}Ga_{0.5}As_{0.5}P_{0.5}$ alloys.

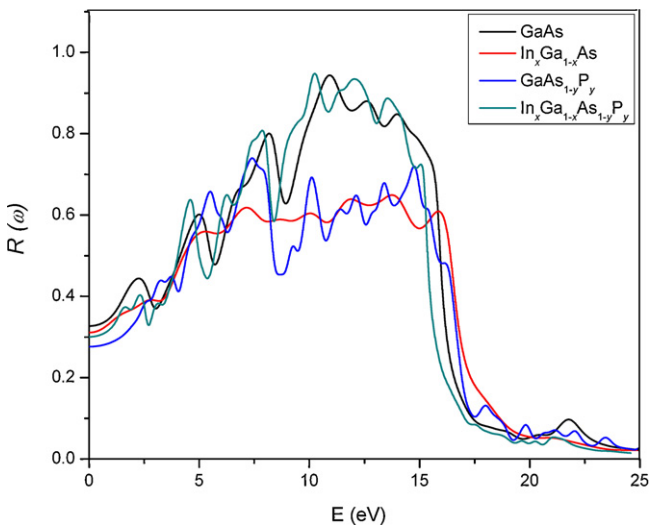

Fig. 9. Optical reflectivity of GaAs, $In_{0.5}Ga_{0.5}As$, $GaAs_{0.5}P_{0.5}$ and $In_{0.5}Ga_{0.5}As_{0.5}P_{0.5}$ alloys.

the figure, this increase in reflectivity decreases at intervals around 7.0–10 eV for these structures. The region between 8 and 13 eV is the reflectivity region for structures. However, it is possible to say that this energy range changes depending on the structure, and there is a deviation in the reflectivity region, especially, of $GaAs_{0.5}P_{0.5}$ and $In_{0.5}Ga_{0.5}As_{0.5}P_{0.5}$ structures. We have monitored this in the components of dielectric function.

4. Conclusions

In summary, we have presented structural, electronic and optical properties of the $In_xGa_{1-x}As$, $GaAs_{1-y}P_y$ ternary and $In_xGa_{1-x}As_{1-y}P_y$ quaternary alloys using the first-principles calculation based on the plane-wave pseudo-potentials method within the LDA approximation. Specifically, the lattice constants, bulk modulus, energy band gap and DOS have been calculated. For all compositions these alloys are characterized by direct and $GaAs_{1-y}P_y$ $y \geq 0.50$ indirect band gap materials along the Γ direction. The starting values of absorption for GaAs, $In_{0.5}Ga_{0.5}As$, $GaAs_{0.5}P_{0.5}$ and $In_{0.5}Ga_{0.5}As_{0.5}P_{0.5}$ alloys semiconductor alloys are 1.43, 0.50, 1.80 and 1.31 eV respectively. The considered optical properties are consistent with the available experimental findings. We hope that some of our results will be tested, to confirm their reliability, in future theoretically experiments and with different methods.

Acknowledgements

The authors would like to thank Profs. Mehmet Kasap, Mahir Bulbul and assistant researcher Murad Sherzad Othman for their assistance in suggestions and discussions. This work is supported by Scientific and Technical Research Council of Turkey (TUBITAK).

References

[1] M. Passlack, N. Medendorp, R. Gregory, D. Braddock, Appl. Phys. Lett. 83 (2003) 5262.
[2] M. Passlack, M. Hong, J.P. Mannaerts, R.L. Opila, S.N.G. Chu, N. Moriya, F. Ren, J.R. Kwo, IEEE Trans. Electron. Device 44 (1997) 214.
[3] H-S Kim, I. Ok, M. Zhang, F. Zhu, Appl. Phys. Lett. 93 (2008) 062111.
[4] J.J. Rosenberg, M. Benlamri, P.D. Kirchner, J.M. Woodall, G.D. Pettit, IEEE Electron. Device Lett. (EDL) 6 (1985) 491.
[5] S.Q. Wang, H.Q. Ye, Phys. Rev. B 66 (235) (2002) 111.
[6] V. Smokal, B. Derkowska, R. Czaplicki, Opt. Mater. 31 (2009) 522.
[7] B. Derkowska, F. Firszt, B. Sahraoui, A. Marasek, M. Kujawa, Opto-Electron. Rev. 16 (2008) 11.

[8] V. Smokal, R. Czaplicki, B. Derkowska, O. Krupka, A. Kolendo, B. Sahraoui, Proceedings of ICTON Miditerranean Winter Conference 2007 (ICTON-MW 2007) IEEE Cat. No: CFP0733D-CDR, 2007, ISBN 978-1-4244-1639-4, pp. 1–4.
[9] B. Sahraoui, S. Dabos-Seignon, A. Migalska-Zalas, Opto-Electron. Rev. 12 (2004) 405.
[10] B. Derkowska, B. Sahraoui, X. Nguyen Phu, C. Andraud, Acta Phys. Pol. A 99 (2001) 165.
[11] B. Derkowska, B. Sahraoui, X. Nguyen Phu, G. Glowacki, W. Bala, Opt. Mater. 15 (2000) 199.
[12] B. Sahraoui, R. Chevalier, G. Rivoire, W. Bala, J. Appl. Phys. 80 (1996) 4858.
[13] J.C. Campbell, N. Holonyak, Phys. Rev. B 9 (1974) 4314.
[14] I.V. Urgaftman, J.R. Meyer, J. Appl. Phys. 89 (2001) 11.
[15] J. Singh, Cambridge University, Cambridge (2003) 27.
[16] F.H. John, Phys. Rev. Lett. 58 (1987) 49.
[17] K. Kim, A. Zunger, Phys. Rev. Lett. 86 (2001) 2609.
[18] B. Geller, W. Wolf, S. Picozzi, A. Continenza, Appl. Phys. Lett. 79 (2001) 368.
[19] M.D. Segall, P.J.D. Lindan, M.J. Probert, C.J. Pickard, P.J. Hasnip, J. Phys. Condens. Matter 14 (2002) 2717.
[20] W. Kohn, L.J. Sham, Phys. Rev. 140 (1965) 1133.
[21] T. Liou, Ch. Yang Lin, S. Yen, Opt. Commun. 249 (2005) 217.
[22] B.K. Agrawal, J. Phys. Condens. Matter 9 (1997) 176.
[23] M.C. Payne, M.P. Teter, D.C. Allen, T.A. Arias, J.D. Joannopolous, Rev. Mod. Phys. 64 (1992) 1045.
[24] H.J. Monkhorst, J.D. Pack, Phys. Rev. B 13 (1976) 5188.
[25] M. Oloumi, C.C. Matthai, J. Phys. Condens. Matter 2 (1990) 5153.
[26] M. Hu Huang, W.Y. Ching, Phys. Rev. B 47 (1993) 15.
[27] O. Stier, M. Grundmann, D. Bimberg, Phys. Rev. B 59 (1999) 8.
[28] K.H. Hellwege, O. Madelung, Landolt-Bornstein. Semiconductors: Physics of Group IV Elements and III–V Alloys, New Series, Group III, (1982), 17.
[29] P. Durmus, A. Uzel, S.Ş. Çetin, S. Özçelik, Balkan, Phys. Lett. 1301 (2008) 8329.
[30] A. Alahmary, N. Bouarissa, A. Kamli, Physica B 403 (2008) 1990.
[31] L. Bellaiche, S.H. Wei, A. Zunger, Phys. Rev. B 57 (1998) 4425.
[32] Q. Wang, X. Ren, H. Huang, Y. Huang, S. Cai, Microelectron. J. 40 (2009) 87.
[33] J. Ishihara, A. Nakamura, S. Shigemori, T. Aoki, J. Temmyo, Appl. Phys. Lett. 89 (2006) 091914.
[34] D. Bedeaux, J. Vlieger, Optical properties of Surfaces, World Scientific Publishing, USA, 2001, p. 444s.
[35] W.F. Smith, Principles materials science and engineering, McGraw-Hill, Inc, USA, 1990, p. 864s.
[36] T. Liu, J. Chen, F. Yan, J. Lumin. 129 (2009) 104.
[37] D. Hăsko, J. Electron. Eng. 3 (2007) 176.
[38] P. Bhattacharya, Properties of Lattice-Matched, Strained Indium Gallium Arsenide London, The Institution of Electrical Engineers, 1993.
[39] M. Hass, B.W. Henvies, J. Phys. Chem. Solids 23 (1962) 1099.
[40] F. Wooten, Optical Properties of Solids, Academic, New York, 1972.
[41] H. Akkuş, A.M. Mamedov, J. Phys. Condens. Matter 19 (2007) 116207.
[42] H.Q. Ni, Z.C. Niu, Appl. Phys. Lett. 84 (2004) 25.
[43] H-C Kuo, Y-H Chang, J. Selected Top. Q. Elect. 11 (2005) 12.
[44] T.J. Kim, T.H. Ghong, Y.D. Kim, Phys. Rev. B 68 (2003) 115323.
[45] J. Tragardh, A.I. Persson, J. Appl. Phys. 101 (2007) 123701.
[46] N. Serpone, D. Lawless, R. Khairutdinov, J. Phys. Chem. 99 (1995) 16646.